

Development and Application of a Downhole Corrosion Prediction Model

Sonja Richter, Mohsen Achour
ConocoPhillips
Bartlesville, OK 74004
USA

Kyle Addis, Marc Singer, Srdjan Nesic
Institute for Corrosion and Multiphase Technology
Ohio University
Athens, OH 45701
USA

ABSTRACT

Corrosion models used in the oil and gas industry are generally aimed at conditions found in pipelines and topside facilities at moderate temperatures and pressures where ideal behavior and solubility for gases can be assumed. The conditions downhole in wells can be very different, inherently at high temperatures and pressures, especially in deep wells. Ideal gas and liquid behavior no longer applies. A corrosion model was developed to take into account the non-ideality that can be found in production through downhole tubing. In this model, Peng-Robinson equation of state replaces the ideal gas assumption, and fugacity is used rather than partial pressures. Henry's law was replaced by Duan's models to calculate solubility of CO₂ and H₂S for higher range of temperatures and pressures. Furthermore, the Pitzer activity model is used to account for non-ideality of the concentration of ionic species in the water phase. The model was tested against lab data, compared with other corrosion models and then finally to field experience. The model shows an improvement from similar models that don't take non-ideality into an account and it can provide the user with increased understanding of downhole corrosion. The interface is adapted for common well data and is user friendly.

Key words: downhole, CO₂/H₂S corrosion, HPHT, corrosion model, production tubing, oil & gas

INTRODUCTION

Carbon dioxide (CO₂) and hydrogen sulfide (H₂S) corrosion are a significant issue in oil and gas production and transportation systems. Modeling has contributed a great deal in understanding and mitigating corrosion. Until now, it has been common practice among operators to use the de Waard-Milliams correlation for corrosion prediction.¹¹ However, this correlation is not intended for well applications and is not valid in the range of environmental parameters encountered in well conditions like high pressures and temperatures, presence of H₂S, etc. Consequently, there is a need to develop better

prediction tools. Many of the models used in the oil and gas industry for corrosion rate prediction are based on laboratory and field data at transport pipeline conditions (<80°C, <20 bar).¹²⁻¹⁵ This includes the mechanistic corrosion prediction model FREECORP⁽¹⁾, called “PONT MODEL” in the text below. As the POINT MODEL was based on an electrochemical model of corrosion¹² and was developed for relatively low temperatures and pressures when compared to downhole conditions, it doesn’t account for factors such as non-idealities and corrosion product stability. Thus, an improved model was developed for production tubing corrosion, known as WELLCORP⁽²⁾, called “WELL MODEL” presented in this paper, by modifying the POINT MODEL to predict corrosion rates and corrosion products for production tubing conditions.

Modeling Corrosion

One of the first attempts at modeling the CO₂ corrosion process was performed by de Waard and Milliams.^{16,17} They suggested a simple means to calculate corrosion rate from temperature and partial pressure of CO₂ using a simple equation or nomogram. This was expanded upon by de Waard *et al.* to include effects of additional factors including flow and pH.^{18,19} Even if the original model was rooted in theory, the subsequent models de Waard *et al.* were semi-empirical. This empiricism restricted these models to application within a very limited range of conditions and parameters for which they were calibrated.

In 1996, Netic *et al.* proposed a mechanistic model, which not only took into account the above mentioned parameters, but also incorporated the contribution of chemical/electrochemical reactions.¹² This model was later updated to include H₂S corrosion.^{10,11} It also assumes an ideal gas phase, which is not suitable for the high temperatures and pressures that are present in downhole corrosion.

In 2003, Nordsveen *et al.* and Netic *et al.*¹³⁻¹⁵ introduced an advanced model which included the diffusion of species, electromigration, and precipitation of surface layers. This model took into account the formation of surface layers, which allowed for a more accurate prediction of corrosion rates in film forming conditions. This model was modified and expanded over the years to include the effects of organic acids, H₂S, high salt, low temperatures, multiphase flow, top of the line corrosion (TLC), etc. The line version of this model is known as MULTICORP⁽³⁾. However, it is still not suitable to predict downhole corrosion rates properly; this is due to the model being calibrated with laboratory data at relatively low temperatures and pressures and assuming ideal behavior. From this point forward in the text, this model is referred to as the “PIPELINE MODEL”.

Parameters Affecting Production Tubing Corrosion

Production tubing refers to the steel tubular connecting the reservoir and the wellhead at the surface. The tubing near the reservoir is often exposed to high pressure and high temperature, of the order of 150°C and 500 bar or even greater.²³ These conditions vary from well to well and over time as wells become depleted – the pressure in the well decreases. In addition, the composition of each well can vary greatly, with some gas wells mostly containing acid gases (i.e. CO₂ and H₂S) while others may be mostly hydrocarbons. In the following sections, some of the important factors affecting production tubing corrosion are discussed.

Volumetric Flow Rates

⁽¹⁾ Free open source corrosion prediction software developed by the Institute for Corrosion and Multiphase Technology, Ohio University (available at <http://www.corrosioncenter.ohiou.edu/freecorp>)

⁽²⁾ Well Corrosion prediction software developed by the Institute for Corrosion and Multiphase Technology, Ohio University

⁽³⁾ Prediction software for CO₂/H₂S corrosion developed by the Institute for Corrosion and Multiphase Technology, Ohio University

The volumetric flow rates of oil, gas, and water are important parameters for calculating the velocity of each phase. The water velocity has a direct impact on the extent of corrosion.²⁴ Additionally, high liquid velocities can lead to the removal of corrosion product layers and if sand is present - erosion.^{14,25} The gas flow rate is also used in calculating the amount of water that condenses along the tubing. Volumetric flow rates are commonly and accurately measured parameters, since they have a direct impact on the profit of the producer.

Flow Regime

The flow regime is another factor that can have a drastic effect on corrosion rates.²⁶ It is suggested that flow can transition between a variety of flow regimes during the ascent up the tubing.²⁷ There are three common flow regimes seen in downhole tubing: bubbly, slug (intermittent), and annular mist. In bubbly flow, the pipe is filled with liquid that contains many dispersed bubbles. If there are intermittent pockets of large gas bubbles pushing the liquid phase, then this is referred to as slug flow. The last case, annular mist flow takes place when the liquid phase flows near the wall of the pipe and the gas phase with small droplets flows through the center. The type of flow regime affects the thickness and velocity of the water layer flowing up the tubing and, therefore, the corrosion through the mass transfer and wall shear stress at the steel surface. Additionally, if crude oil is present, this can have a dramatic impact on the corrosion rate of the system due to the water/oil wetting effects as well as inhibition effects provided by crude oil.^{11,38}

Brine Composition

The brine composition is an important parameter, but it is often not reported for wells. It is, however, key to making accurate corrosion prediction. This is because the composition of the produced water affects the way in which aqueous species interact with each other and the pipe wall. For example, high concentrations of salt (typically chlorides) can be detrimental to corrosion resistant alloys (CRA) but can lead to a decrease in corrosion rate of mild steel.²⁸ Since some fields can have upwards of 200,000 ppm of chlorides in the produced waters²³, this needs to be accounted for in the model.

The acidity/basicity of the brine is often specified in term of alkalinity, as in-situ pH cannot be directly measured accurately in the well. Total alkalinity is an important factor in pH calculations, and represents the amount of acid required to neutralize the produced water from the well. It is usually measured in a lab by titration; the pH endpoint can vary depending on the procedure and indicator used, but typically, it is around pH 5.1 and pH 4.5.²⁹ This provides a quantification of the acid reducing power of the produced water and generally is reported as bicarbonate equivalent (HCO_3^-). Often, there is organic acid present in the brine, which even at low concentrations can have a major impact on the corrosion rate.²⁰

Gas Composition

The composition of the gas stream has probably the largest impact on the corrosion inside a well. At the very minimum, the concentration of CO_2 and H_2S should be reported, but if the full composition of gas is provided; a more accurate characterization of the well is possible. The partial pressures of CO_2 and H_2S directly influence the concentration of corrosive species in solution and thus corrosion rates inside the tubing.^{20,31} Some fields are highly sour, upwards of 20 percent or more, in addition to having already high concentrations of CO_2 , e.g. 40 mol% or more.²³ The other inert species, such as methane, ethane, and nitrogen, affect the gas molecular weight and density. These two parameters in turn affect the gas velocity, and the flow regime.

Temperature and Pressure

Temperature has been shown to be an important factor in the corrosion process and was one of variables included in the original de Waard-Milliams model.^{16,17} High temperatures will generally lead to higher corrosion rates, given that no corrosion product layer forms.^{28,32} Additionally, the flowing bottomhole and wellhead temperatures are important for determining not only the temperature gradient, but also many

other physical properties of the fluid along the length of the well. Temperature has an effect on the phase densities, acid gas solubilities, and corrosion product formation.³³ If the temperature is high enough, a protective corrosion product layer can form composed of iron carbonate (FeCO_3) and/or magnetite (Fe_3O_4), lowering corrosion rate significantly.³⁴ In the presence of H_2S , an iron sulfide layer is typically present.^{35,1}

Total pressure alone has little effect on the corrosion process, but it is directly related to the partial pressures of CO_2 and H_2S , which have a major influence on the corrosion rate.^{32,2} The flowing bottomhole and wellhead pressures are used for calculating the pressure gradient along the tubing and for following the change in partial pressures along the well. Pressure also affects the gas phase density and in turn has an effect on the gas velocity.

Tubing sizing and properties

The tubing inner diameter is used to convert the volumetric flow rates to velocities. The length of the tubing is used to calculate temperature and pressure profiles. In addition to the dimensions of the tubing, the properties, and the composition of the tubing are also important. Carbon steels and corrosion resistant alloys (CRAs) will obviously have different corrosion behavior. In the presence of H_2S , harder steels may be susceptible to sulfide stress cracking; thus, a nickel-based alloy such as Hastelloy C-276 may be needed.³⁶ The materials used for downhole tubing and casing are subject to the NACE MR0175 standard³⁷, which provides guidance on material hardness and yield strength. All field data used in this work are from fields using API L-80, J-55, and J-65 steels. Most laboratory experimental data are obtained using X-65 steel.

Key Challenges in Modeling Production Tubing Corrosion

Harsh Conditions

Conditions in wells are often much harsher than those in the transportation lines.²³ In addition, a wider range of operational conditions can be encountered. Temperatures can range from near freezing at the wellhead to well beyond 100°C , depending on the geographic location and depth of the well. Corresponding pressures can range from just above atmospheric pressure, up to 700 bars and more. Not only does the high end of pressures and temperatures pose problems for modeling, but also the wide range of conditions that need to be modeled.

Non-idealities

At some of the extreme well conditions mentioned above, the gas phase does not act in an ideal manner due to interactions at the molecular level. Thus, a more robust equation of state is required to perform the calculations, replacing the ideal gas law. Pressures are converted to fugacities, or an effective pressure, to account intermolecular interactions.^{3,40} In addition to the non-idealities in the gas phase, there are also non-idealities in the produced water. These non-idealities arise due to the high concentrations of salt ions in the produced water, which is caused by the interaction of species in the solution. To take into account this issue, concentrations must be converted into activities, or the effective concentrations.^{4,41,42}

Lack of accurate data

The final challenge related to wells is related to the overall accuracy of the data available. Production rates are averaged rates, either on a daily or monthly basis, so periods of high and low production can be missed. The composition of the produced water and gas phase may only be measured once or few times during the lifetime of the well.⁴³ These compositions could change greatly with the lifetime of the well. The pressure and temperature profile must also be estimated, since the true profile is not always available. In this case, they are assumed to change linearly along the tubing. Additionally, pH must be estimated from alkalinity, since it cannot be directly measured. There have been recent attempts by

Plennevaux *et al.*⁴⁴ to improve pH calculations at downhole conditions by making use of a modified Henry's law, however, this can still be improved upon.

In addition to the inaccuracy related to production data, the wall losses reported by in-line inspection techniques are often quite inaccurate. The accuracy of caliper data is often around 70-80%.⁴⁵ More accurate techniques are available for transport lines, but because of the inherent design of production tubing, the only available technique for wall loss measurement is a caliper survey.

This review of the current state of the art in has shown that there are many complexities associated with production tubing corrosion that are unaccounted for by the present models¹². The objective of the present work is to address some of these complexities and to compare the improved model with field and experimental data.

WELL MODEL DESCRIPTION

The WELL MODEL has a user friendly interface as seen in Figure 1. The inputs are on the left hand side (white boxes), and the output is on the right. The user can change the units, either from a drop-down menu for each input or globally by selecting the appropriate radio button on top. All the essential inputs needed to run the model are given in the main user interface, but in addition, the user has three *Advanced Options*. The *Gas Input* tab allows the user to calculate the molecular weight of the gas from the gas composition, the *Brine Input* tab allows the user to calculate the ionic strength based on the water chemistry, and the *Flow Model* tab allows the user to either specify or calculate the flow pattern.

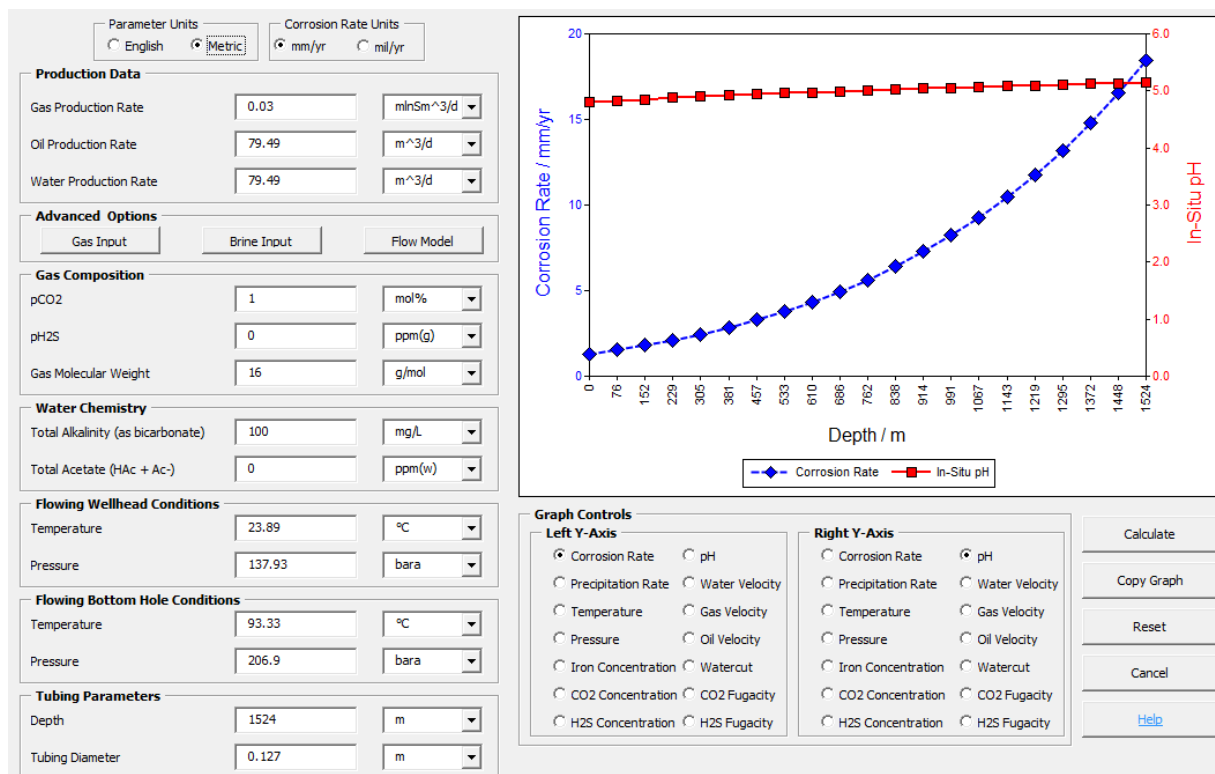


Figure 1: Interface of the WELL MODEL, showing inputs on the left hand side and output on the right.

The output is graphed on the right hand side with the well head conditions towards the left (0m for depth) and the bottom hole conditions towards right. The user can select different outputs from the list below the graph. In addition, the model gives the inputs and some of the outputs, including the corrosion products (e.g., FeCO₃, FeS) and flow patterns, in a spreadsheet format.

The POINT MODEL¹², which constitutes the starting point of this new modeling effort, suffers from a number of limitations which makes it ill suited for modeling of well conditions. The POINT MODEL calculates a corrosion rate based on one single set of input data (hence the name “point model”), it assumes simple single-phase flow, i.e. a pipe filled entirely with water, and it uses Henry’s law to calculate CO₂ and H₂S aqueous concentrations from gas composition data.

A discussion of the new features added in the development of the WELL MODEL is presented in the following sections, stressing the points of improvement as compared to the POINT MODEL. The key new features include: a line model corrosion prediction (along the well length), introduction of fugacity coefficients, activity coefficients, and a new flow model.⁴⁵

Corrosion – Point Model

As stated above, the corrosion model in the WELL MODEL is based on the POINT MODEL. The electrochemical method for calculating corrosion rates is left largely the same as presented in the original paper¹² and only a very brief description is presented here. Anodic and cathodic current densities are expressed as function of the corrosion potential which is obtained by solving the charge balance using Equation (1).

$$i_{c(H^+)} + i_{c(H_2CO_3)} + i_{c(HAc)} + i_{c(O_2)} + i_{c(H_2O)} = i_{a(Fe)} \quad (1)$$

where,

- i_c is the total cathodic current density for a species, A/m²;
- i_a is the total anodic current density for a species, A/m²;

The equation enabling the calculation of the corrosion rate CR is obtained using the current density of the anodic iron dissolution reactions i_{corr} . Equation (2) shows how this current density is converted to the corrosion rate.

$$CR = \frac{i_{corr} M_{Fe}}{\rho_{Fe} n F} \quad (2)$$

where,

- M_{Fe} is the molar mass of iron, g/mol;
- ρ_{Fe} is the density of iron, g/m³;
- n is the number of electrons released ($n=2$ for iron oxidation);
- F is the Faraday’s Constant.

Corrosion – Line Model

The original POINT MODEL is a model where for one set of conditions only one corrosion rate is calculated. However, to accurately simulate corrosion in production tubing, multiple points (control volumes) along the tubing must be simulated, thus a line model is needed. Additionally, the conditions at this set of points are related as the flow carries the corrosion products downstream from one point to the next. To link the points together, a mass balance is performed on the ferrous ions in the system, as shown by Equation (3). Thus, corrosion at the lower end of the tubing has an impact on the corrosion calculated at points above it.

$$C_{Fe^{2+}_{out}} = C_{Fe^{2+}_{in}} + \frac{((CR - PR) * \rho_{Fe} * A_p)}{(M_{Fe} * A_c * v)} \quad (3)$$

where,

- $c_{Fe_{out}^{2+}}$ is the concentration of Fe^{2+} exiting the control volume, mol/m³;
- $c_{Fe_{in}^{2+}}$ is the concentration of Fe^{2+} entering the control volume, mol/m³;
- CR is the average corrosion rate at the control volume, m/yr;
- PR is the average precipitation rate, m/yr;
- ρ_{Fe} is the density of iron, kg/m³;
- A_p is the surface area of pipe, m²;
- M_{Fe} is the molecular mass of iron, mol/m³;
- A_c is the cross-section area of pipe, m²;
- v is the velocity of fluid, m/s.

Non-Idealities

Gas phase non-idealities are corrected by using fugacity, while liquid phase non-idealities are corrected by using activities. These improve the accuracy of the gas solubility model and pH prediction.

Fugacity

Fugacities in the WELL MODEL are calculated using the Peng-Robinson equation of state.⁵ By using Equations (4) and (5), the individual fugacity for a species can be calculated for a gas mixture. This correction accounts for the intermolecular interactions that occur at high pressures.

$$\ln \frac{f_k}{x_k p} = \frac{b_k}{b} (Z - 1) - \ln(Z - B) - \frac{A}{2\sqrt{2}B} \left(\frac{2 \sum_i X_i a_{ik}}{a} - \frac{b_k}{b} \right) \ln \left(\frac{Z + 2.414B}{Z - 0.414B} \right) \quad (4)$$

$$a_{ik} = \sqrt{a_i a_k} (1 - k_{ik}) \quad (5)$$

where:

- k is the k -th component in the mixture;
- i is the i -th component in the mixture;
- x is the mole fraction;
- a_{ik} is the binary interaction parameter.

Activity

The Pitzer activity model is used in the WELL MODEL to correct for the high salinity experienced in oil and gas production^{6,7}. The high concentrations of salts can lead to ions interacting within the solution, thus changing the effective concentrations. To account for this, an activity coefficient is needed. Equations (6) and (7) show the Pitzer activity model used in the WELL MODEL.

$$\ln \gamma = |z_M z_X| f^\gamma + m \left(\frac{2v_M v_X}{v} \right) B_{MX}^\gamma + m^2 \frac{2(v_M v_X)^{3/2}}{v} \left(\frac{3}{2} \right) C_{MX}^\varphi \quad (6)$$

where:

- γ is the activity coefficient;
- z_M is the charge of species M ;
- z_X is the charge of species X ;

f^{ν} is defined in Equation 41;
 m is the molality, mol/kg solvent;
 ν_M is the number of M ions in the formula;
 ν_X is the number of X ions in the formula;
 ν is the sum of ν_M and ν_X ;
 B_{MX} is the empirical correction for ionic strength;
 C_{MX} is the empirical factor for each species;
 f^{ν} is defined as:

$$f^{\nu} = -A_{\varphi} \left[\frac{I^{1/2}}{1 + bI^{1/2}} + \frac{2}{b} \ln(1 + bI^{1/2}) \right] \quad (7)$$

where:

A_{φ} is the Debye-Hückel coefficient;
 b is the constant equal to 1.2.

Acid Gas Solubility Models

The CO₂ and H₂S solubility models used in the WELL MODEL are based on the semi-empirical models of Duan.^{8,9} These two models are based on the virial equation of state and have been fitted to solubility data from literature. Both models also take in to account the effects of salt ions on the solubilities of CO₂ and H₂S. The CO₂ model is valid up to 2000 bars pCO₂ and 260°C, while the H₂S model is valid up to 200 bars pH₂S and 227°C. These improved solubility models show significant improvement over the Henry's Law correlations used in the POINT MODEL.

Flow Model

To overcome the limitation of specifying flow conditions in the POINT MODEL a mechanistic multiphase flow model¹⁰ was added to the WELL MODEL. The model is capable of predicting flow patterns and calculating in-situ velocities, among other features.

The in-situ liquid velocity is the most important output from the flow model as this is fed into the flow factor calculation. The POINT MODEL uses water velocity to calculate the mass transfer coefficient used in calculation of diffusion limiting currents for cathodic species such as hydrogen ions and to calculate the theoretical flow factor for the carbonic acid reduction reaction. The flow factor has an effect on the CO₂ hydration reaction, and thus is present in the limiting current calculation for carbonic acid as shown by Equation (8).

$$i_{lim,H_2CO_3} = F c_{CO_2} (\eta_{FeCO_3} \eta_{FeS} D_{H_2CO_3} K_{hyd} k_{hyd}^f)^{0.5} f \quad (8)$$

Where:

c_{CO_2} is the concentration of CO₂ in the bulk solution, mol/m³;
 η_{FeCO_3} , η_{FeS} are the scale factors for FeCO₃ and FeS respectively;
 $D_{H_2CO_3}$ is the diffusion coefficient of carbonic acid in water, m²/s;
 K_{hyd} is the equilibrium constant for carbon dioxide hydration reaction;
 k_{hyd}^f is the forward reaction rate constant for carbon dioxide hydration reaction;
 f is the flow factor affecting carbon dioxide hydration.

RESULTS

Part of the development of the WELL MODEL consisted of validating the model against lab and field data.³⁵ In this paper, three (3) field cases are considered for demonstrating the capabilities and the advantages of the WELL MODEL. The conditions for each case is given in Table 1 and the water chemistry for case 2 and case 3 is given in Table 2. A thermodynamic software called THERMOCORP⁽⁴⁾ (called “POURBAIX MODEL” in the text below) is used to determine the stability of surface corrosion product layers, such as iron carbonate (FeCO₃), magnetite (Fe₃O₄), etc., from generated Pourbaix diagrams.

Table 1
Conditions for the Field Cases

	Case 1	Case 2	Case 3
Gas Flow Rate (Sm ³ /d)	17,610	36,500	2435
Water Flow Rate (m ³ /d)	0.06	1.6	188
Oil Flow Rate (BPD)	0.5	0	16.5
Well Head Temperature (°C)	10	12	40
Well Head Pressure (bar)	7.6	8.7	9.7
Bottom Hole Temperature (°C)	90 / 93	49	105
Bottom Hole Pressure (bar)	13	41	240
pCO ₂ (mol%)	1.92	1.5	1.45
Gas Molecular Weight (g/mol)	21	17.18	21.2
Bicarbonate (ppm)	68	568	100
Depth (m)	2806	1070	1524
ID (m)	0.05	0.06	0.05

Table 2
Water Chemistry for the Field Cases

	Case 2	Case 3
Chloride (ppm)	1440	-
Sulfate (ppm)	<4	-
Barium (ppm)	4.75	1.4
Calcium (ppm)	67.2	196.2
Iron (ppm)	49.3	2.1
Magnesium (ppm)	21.6	330.8
Potassium (ppm)	67.3	-
Sodium (ppm)	1030	-
Strontium (ppm)	8.83	-

⁽⁴⁾ Thermodynamic prediction software developed by the Institute for Corrosion and Multiphase Technology, Ohio University

Case 1: Investigating the Failure Mechanism

This case is from a field with about two dozen wells that are plunger-lifted and produce sweet gas, all from the same formation. The wells had not been inhibited since they started production in 2002-2003. However, in the years 2013 – 2015, they've had 1-2 tubing repairs per year on three of the wells due to corrosion.

Figure 2 shows the results of a simulation for one of the wells (see Table 1 for the conditions used for the simulation). There two variations are shown – when the bottomhole temperature (BHT) is 93°C and 90°C. When a simulation is made at a slightly lower BHT (90°C), the corrosion rate in the bottom half of the tubing becomes higher compared to the corrosion rate at the slightly higher BHT. This difference (higher corrosion rate at a lower temperature) is due to the fact that the conditions for which the simulation is executed fall very close to the transition between bare steel corrosion (Fe^{2+} stable in the Pourbaix diagram shown in Figure 3) and iron carbonate formation (FeCO_3 stable in the Pourbaix diagram shown in Figure 3). Slightly higher BHT (93°C) predicts a pH just above pH6 and the corrosion rate is calculated assuming iron carbonate is forming. However, the lower BHT (90°C) results in pH just below 6, and the corrosion rate is calculated assuming bare steel corrosion. In reality, the transition between film free and iron carbonate conditions is not so dramatic, therefore, it can be expected that the surface is partially covered with iron carbonate, what may compromise the protection and even lead to localized corrosion.

Interestingly, both cases (bare steel corrosion and iron carbonate covered steel) result in similar corrosion rates at the top half of the tubing, down to a depth of circa 1500 m. Beyond that point the bare steel corrosion rates become increasingly higher and are about 3 mm/y at the bottom, while the corrosion rates assuming iron carbonate formation are about 1 mm/y. The wells would typically fail at 1700 m depth (dashed line in Figure 2), which is at the location when the pH is predicted to drop below pH6. Therefore, it can be assumed that the wells are failing because a poorly protective iron carbonate layer with only a partial coverage on the tubing surface creates conditions that favor pitting where the unprotected surface is surrounded with iron carbonate layer.

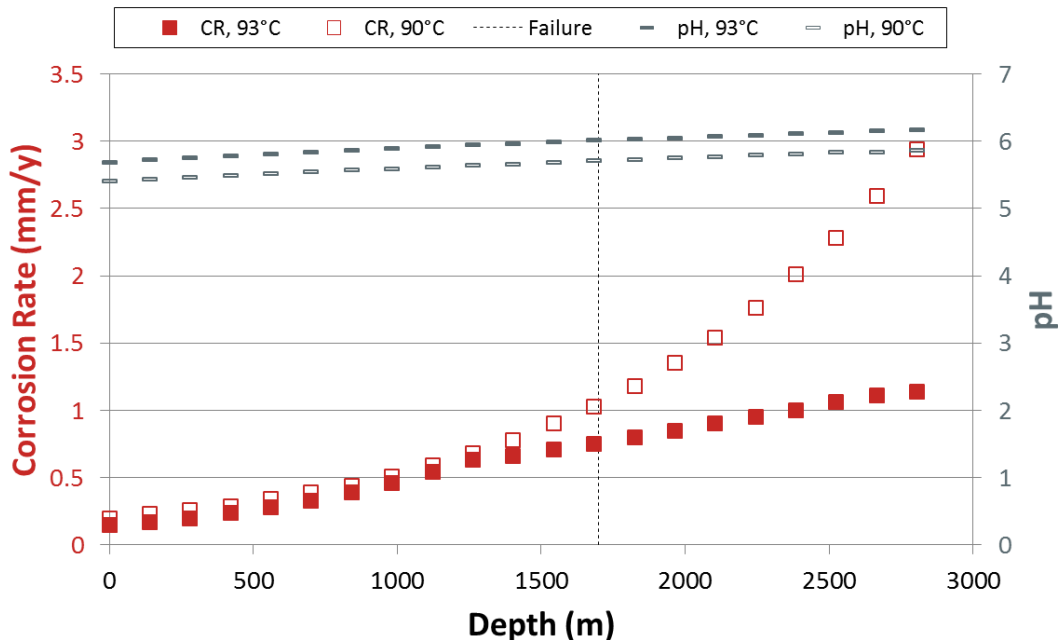


Figure 2: Predicted corrosion rate (CR) shown as red data points on the left y-axis for a BHT of 90°C and 93°C in Case 1. The pH (grey data points) is displayed on the right-hand axis.

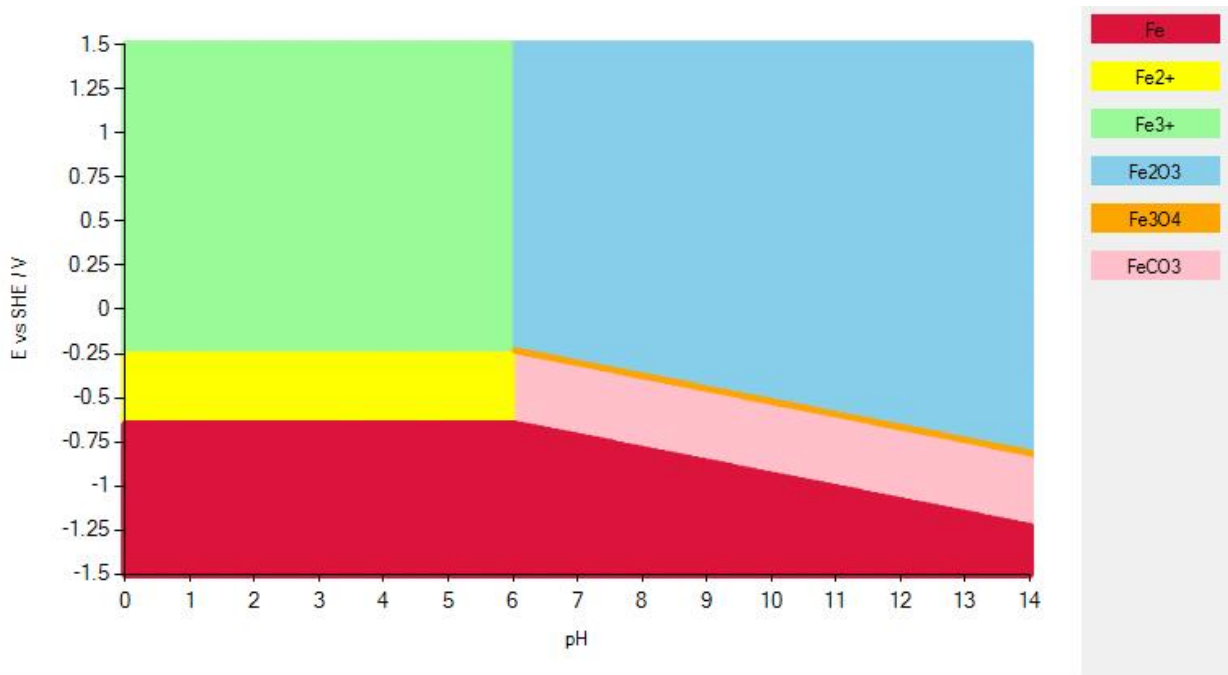


Figure 3: Diagram generated with the POURBAIX MODEL showing transition between bare steel corrosion (Fe^{2+}) and iron carbonate (FeCO_3) at pH6 for Case 1

Case 2: Comparison with Other Models

Being a line model has evident value when evaluating tubing corrosion, where the pressure and temperature is rapidly changing. The WELL MODEL automatically divides the tubing into twenty (20) segments (control volumes) and calculates the corrosion rate for each one of them. Here the results are compared with two other models.

The results of WELL MODEL are similar to the other two models at the top of the well, where pressures and temperature are not so high, but deviate quite a bit from the other two prediction models at bottomhole conditions, where both predicts much lower corrosion rates. Since both the PIPELINE MODEL and POINT MODEL assume ideal conditions, WELL MODEL's predictions are likely to deviate from the other similar models as the temperature and pressure increase further from standard conditions, and this is seen in Figure 4. This does not necessarily mean that WELL MODEL is more accurate, although in this case it does provide more conservative results, which is preferable from operation and asset integrity point-of-view. However, the relatively high concentration of iron (47.9 ppm) in the water chemistry (Table 2) suggest that corrosion is actively occurring. Furthermore, the relatively high amount of bicarbonate (528 ppm) does not seem to be sufficient to ensure iron carbonate formation, perhaps because the water is a low-salt brine. Also, the reduction in corrosion rate predicted for bottomhole conditions by PIPELINE MODEL is due to a very thin and porous FeCO_3 layer taking a long time to form (on the order of days). Therefore, its protectiveness should be questioned and it might even do more harm than good by promoting pitting.

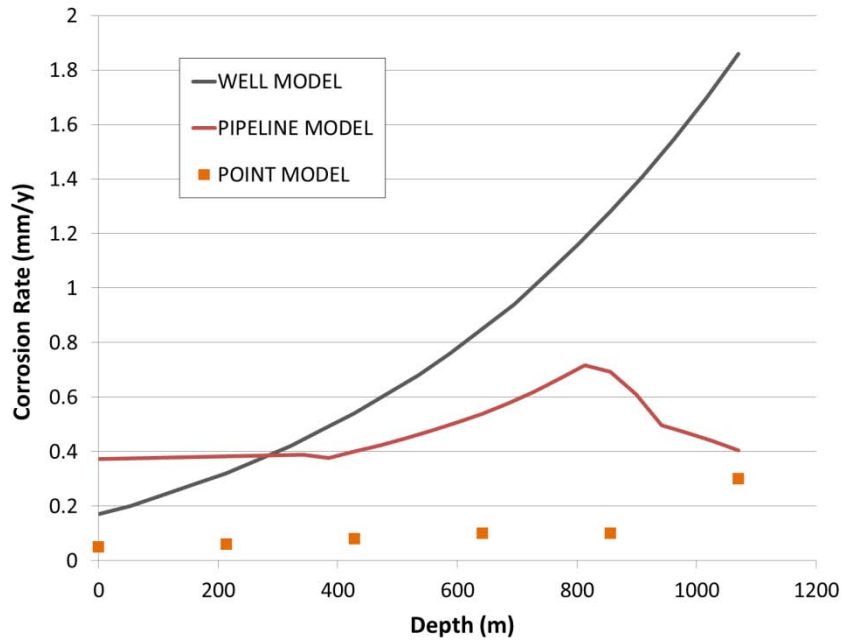


Figure 4: Corrosion Simulation of a well using different software, WELL MODEL (gray), PIPELINE MODEL (red) and POINT MODEL (orange) for Case 2.

Case 3: Mitigation Planning Strategies

While pitting in a flowline or a pipeline can result in a spill causing environmental damage, losing containment of the tubing will generally not have as grave consequence, and often the consequence is no more than decline in production as the leak is contained within the annulus. Therefore, chemical inhibition is not always needed, especially early in the lifetime of the field when little or no water is being produced.

Determining which wells to inhibit, or when to start inhibiting, can be done reactively. In that case the strategy is to wait for wells to fail, or wait for corrosion coupons to show significant corrosion before inhibition is put in place. Often times it is not practical to place coupons on every single well head, particularly when there are hundreds of wells in the area, and by rotating coupons from well head to well head might mean that a well can fail from corrosion damage before inhibition plan is put in place.

Conducting corrosion modeling is a proactive way of determining which wells to prioritize for monitoring and mitigation. The example in Figure 5 shows a prediction where the corrosion rates are high enough to justify inhibition ($\gg 0.1\text{mm/y}$). Furthermore, the results show that it is expected that conditions vary between bare steel corrosion and iron carbonate covered steel corrosion as the temperature and pressure changes up the tubing (red and blue line in the graph). Indeed, when the temperature range in the well is considered (WHT of 40°C to BHT of 105°C) and the pH range (pH5.90 – pH5.94) it can be seen that these conditions follow exactly the transition between bare steel and iron carbonate formation (Figure 6). Figure 5 shows the depth for which iron carbonate is predicted as a blue line (from 0 m to 200 m). However, there is little effect of the iron carbonate on the corrosion rate. Both of these observations (having a transition and not lowering the corrosion rate) indicate that even if iron carbonate is formed, it will not be protective and it can even trigger pitting by partial coverage of the surface. Therefore, this well should be prioritized for both corrosion monitoring (coupons and/or iron/manganese counts) and corrosion inhibition.

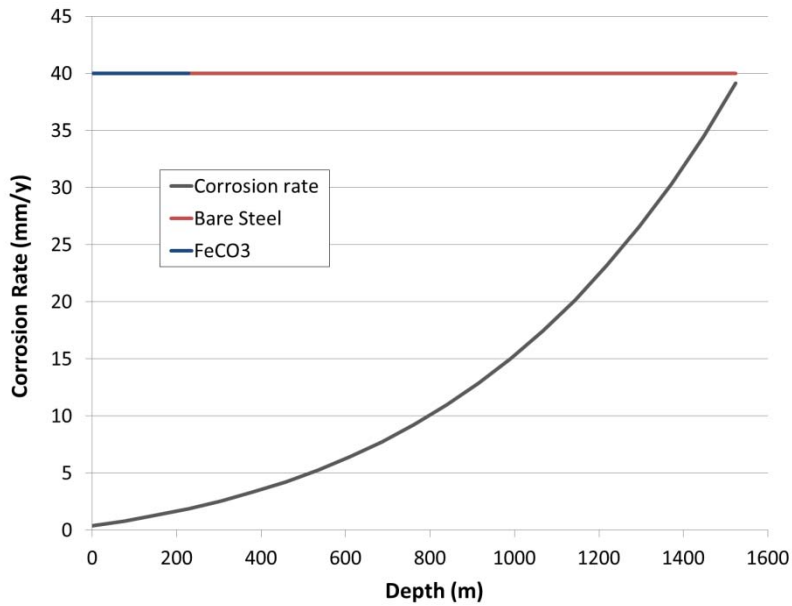


Figure 4: Downhole corrosion rates (gray points) and depths where bare steel corrosion (red line) and iron carbonate formation (blue line) is predicted for Case 3.

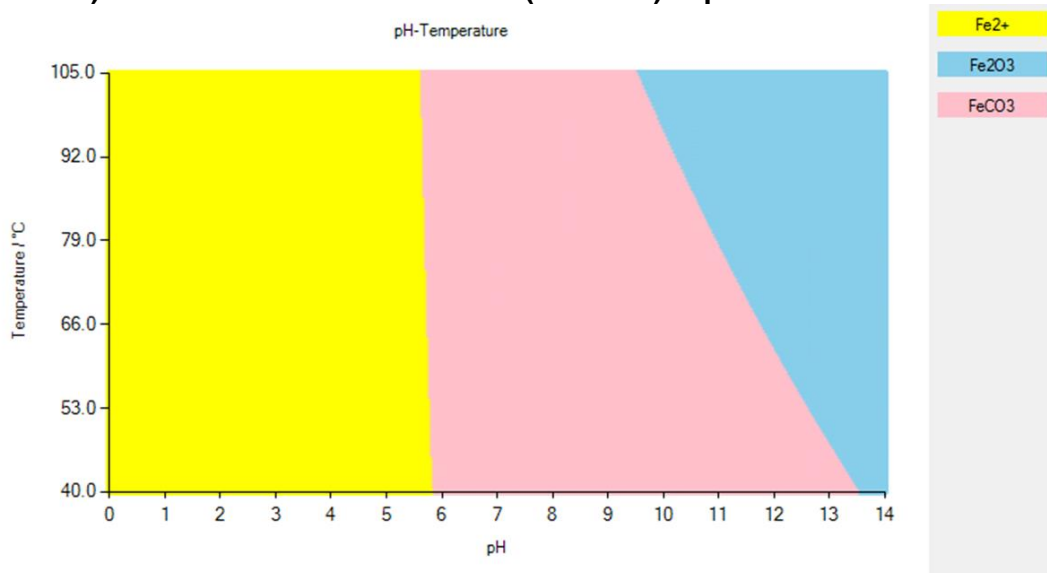


Figure 5: A slice of Pourbaix diagrams at -0.5V from WHT (40°C) to BHT (105°C) produced by the POURBAIX MODEL.

CONCLUSIONS

The WELL MODEL is a corrosion prediction tool that has been developed to predict corrosion in downhole tubing of producing wells. The tool is used for various purposes, including estimation of the tubing's expected lifetime, risk-ranking, to confirm or exclude possible failure mechanisms, to optimize corrosion monitoring and mitigation, etc.

By predicting the corrosion at regular intervals at different depths, a more holistic sense of the corrosion behavior is obtained. By using point models, the user only can predict one point at a time (often only using well head conditions) which will not give the whole picture of the corrosion threat. The WELL MODEL gives information on all the key parameters changing along the tubing string, including pH and

Fe²⁺ concentration, FeCO₃ and FeS saturation profile and precipitation rate, fugacity of CO₂ and H₂S, in-situ fluid velocities, flow pattern, corrosion rate and scaling factor.

The vast majority of the existing corrosion models assume that the ideal gas law is valid, but that assumption does not always hold downhole, particularly not in high-pressure high temperature-wells. WELL MODEL uses fugacity rather than partial pressures and the Duan solubility model rather than Henry's law. This has resulted in more realistic predictions as demonstrated in this paper.

REFERENCES

11. M. B. Kermani, A. Morshed, "Carbon Dioxide Corrosion in Oil and Gas Production—A Compendium," *Corrosion*, 59, 8 (2003): p. 659–683.
12. S. Nestic, J. Postlethwaite, S. Olsen, "An Electrochemical Model for Prediction of Corrosion of Mild Steel in Aqueous Carbon Dioxide Solutions," *Corrosion*, 52, 4 (1996): p. 280–294.
13. M. Nordsveen, S. Nešić, R. Nyborg, A. Stangeland, "A Mechanistic Model for Carbon Dioxide Corrosion of Mild Steel in the Presence of Protective Iron Carbonate Films — Part 1: Theory and Verification," *Corrosion*, 59, 5 (2003): p. 443–456.
14. S. Nešić, M. Nordsveen, R. Nyborg, A. Stangeland, "A Mechanistic Model for Carbon Dioxide Corrosion of Mild Steel in the Presence of Protective Iron Carbonate Films — Part 2: A Numerical Experiment," *Corrosion*, 59, 6 (2003): p. 489–497.
15. S. Nešić, K.-L. J. Lee, "A Mechanistic Model for Carbon Dioxide Corrosion of Mild Steel in the Presence of Protective Iron Carbonate Films — Part 3: Film Growth Model," *Corrosion*, 59, 7 (2003): p. 616–628.
16. C. de Waard, D. E. Milliams, "Carbonic Acid Corrosion of Steel," *Corrosion*, 31, 5 (1975): p. 177–182.
17. C. de Waard, D. E. Milliams, "Prediction of Carbonic Acid Corrosion in Natural Gas Pipelines," First International Conference on the Internal and External Protection of Pipes, paper no. F1 (Cranfield, England: BHRA, 1975): p. 1–8.
18. C. de Waard, U. Lotz, "Prediction of CO₂ Corrosion of Carbon Steel," CORROSION/93, paper no. 69 (Houston, TX: NACE, 1993): p. 1–17.
19. C. de Waard, U. Lotz, A. Dugstad, "Influence of Liquid Flow Velocity on CO₂ Corrosion: A Semi-Empirical model," CORROSION/95, paper no. 128 (Houston, TX: NACE, 1995): p. 1–14.
20. W. Sun, S. Nestic, "A Mechanistic Model of Uniform Hydrogen Sulfide/Carbon Dioxide Corrosion of Mild Steel," *Corrosion*, 65, 65 (2009): p.291-307.
21. Y. Zheng, B. Brown, S. Nešić, "Electrochemical Study and Modeling of H₂S Corrosion of Mild Steel," *Corrosion*, 70, 4 (2014): p. 351–365.
22. S. Nešić, H. Li, J. Huang, D. Sormaz, "An Open Source Mechanistic Model for CO₂/H₂S Corrosion of Carbon Steel," CORROSION/09, paper no. 09572 (Houston, TX: NACE, 2009): p. 1–19.
23. S. N. Smith, R. Pakalapati, "Thirty Years of Downhole Corrosion Experience at Big Escambia Creek: Corrosion Mechanisms and Inhibition," CORROSION/04, paper no. 04744 (Houston, TX: NACE, 2004): p. 1–17.
24. G. Schmitt, B. Rothmann, "Studies on the Corrosion Mechanism of Unalloyed Steel in Oxygen-Free Carbon Dioxide Solutions. Part I - Kinetics of the Liberation of Hydrogen," *Werkstoffe und Korrosion*, 28, (1977): p.816.
25. Y. Yang, B. Brown, S. Nešić, M. E. Gennaro, B. Molinas, "Mechanical Strength and Removal of a Protective Iron Carbonate Layer Formed on Mild Steel in CO₂," CORROSION/10, paper no. 10383 (Houston, TX: NACE, 2010): pp. 1–19.
26. B. Pots, "Mechanistic Models for the Prediction of CO₂ Corrosion Rates Under Multiphase Flow Conditions," CORROSION/95, paper no. 137 (Houston, TX: NACE, 1995): p. 1–20.

27. G. M. Abriam, "Controlling Corrosion of Carbon steel in Sweet High Temperature and Pressure Downhole Environments with the Use of Corrosion Inhibitors," NACE Northern Area Western Conference, (Houston, TX: NACE, 2010).
28. H. Fang, "Low Temperature and High Salt Concentration Effects on General CO₂ Corrosion for Carbon Steel," M.S. thesis, Ohio University, Athens, OH, 2006.
29. J. D. Hem, *Study and Interpretation of the Chemical Characteristics of Natural Water*, 3rd ed. (Alexandria, VA: U.S. Geological Survey, 1985): p. 106.
30. S. Wang, K. George, S. Nešić, "High Pressure CO₂ Corrosion Electrochemistry and the Effect of Acetic Acid," CORROSION/04, paper no. 04375, (Houston, TX: NACE, 2004): p. 1–17.
31. Institute for Corrosion and Multiphase Technology (ICMT), "FREECORP Background." Online publication. Available: <http://www.corrosioncenter.ohiou.edu/software/freecorp/pdfs/FREECORP-Background.pdf>. (Accessed: 26-Mar-2013).
32. S. Nešić, S. Wang, H. Fang, W. Sun, J. K.-L. Lee, "A New Updated Model of CO₂/H₂S Corrosion in Multiphase Flow," CORROSION/08, paper no. 08535, (Houston, TX: NACE, 2008): p. 1–16.
33. W. Sun, S. Nešić, R. C. Woollam, "The Effect of Temperature and Ionic Strength on Iron Carbonate (FeCO₃) Solubility Limit," *Corros. Sci.*, 51, 6 (2009): p. 1273–1276.
34. T. Tanupabrungsun, "Thermodynamics and Kinetics of Carbon Dioxide Corrosion of Mild Steel at Elevated Temperatures," Ph.D. dissertation, Ohio University, Athens, OH, 2013.
35. J. Ning, Y. Zheng, D. Young, B. Brown, S. Nestic, "A Thermodynamic Study of Hydrogen Sulfide Corrosion of Mild Steel," paper no. 2462: (Houston, TX: NACE, 2013).
36. B. D. Craig, "Metallurgy for Oil and Gas Production," in *Practical Oilfield Metallurgy and Corrosion*, 2nd ed., (Denver, CO: PennWell, 1993): p. 131–141.
37. NACE MR0175/ISO 15156 "Petroleum and natural gas industries — Materials for use in H₂S-containing environments in oil and gas production," (Houston, TX: NACE).
38. C. Mendez, S. Duplat, S. Hernandez, J. Vera, "On the Mechanism of Corrosion Inhibition by Crude Oils," CORROSION/01, paper no. 01044 (Houston, TX: NACE, 2001): pp. 1–19.
39. K. Pedersen, P. Christensen "Flash and Phase Envelope Calculations," in *Phase Behavior of Petroleum Reservoir Fluids*, 1st ed., (Boca Baton, FL: CRC Press, 2007): p. 115–140.
40. D.-Y. Peng, D. B. Robinson, "A New Two-Constant Equation of State," *Ind. Eng. Chem. Fundam.*, 15, 1 (1976): p. 59–64.
41. K. S. Pitzer, "Thermodynamics of Electrolytes I. Theoretical Basis and General Equations," *J. Phys. Chem.*, 77, 2 (1973): pp. 268–277.
42. K. S. Pitzer and G. Mayorga, "Thermodynamics of electrolytes II. activity and osmotic coefficients for strong electrolytes with one or both ions univalent," *J. Phys. Chem.*, 77, 19 (1973): p. 2300–2308.
43. R. Nyborg, "Field Data Collection, Evaluation and Use for Corrosivity Prediction and Validation of Models - Part II: Evaluation of Field Data and Comparison of Prediction Models," CORROSION/06, paper no. 06118 (Houston, TX: NACE, 2006): p. 1–15.
44. C. Plennevaux, T. Cassagne, M. Bonis, J. Kittel, F. Ropital, N. Ferrando, M. Fregonese, B. Normand, "Improving pH Prediction for High Pressure and High Temperature Applications in Oil and Gas Production," Corrosion/13, paper no. 2843 (Houston, TX: NACE, 2013): p. 1–14.
45. K. Addis, "A Corrosion Model for Production Tubing," M.S. Thesis, Ohio University, Athens, OH, 2014.
46. Z. Duan, R. Sun, "An Improved Model Calculating CO₂ Solubility in Pure Water and Aqueous NaCl Solutions from 273 to 533K and From 0 to 2000bar," *Chem. Geol.*, 193, 3–4 (2003): p. 257–271.
47. Z. Duan, R. Sun, R. Liu, C. Zhu, "Accurate Thermodynamic Model for the Calculation of H₂S Solubility in Pure Water and Brines," *Energy & Fuels*, 21, 4 (2007): p. 2056–2065.
48. N. Jauseau, "Multiphase Flow Effects on Naphthenic Acid Corrosion of Carbon Steel," Ph.D. dissertation, Ohio University, Athens, OH, 2012.